Room-Temperature Synthesis of Carbon Nanotubes-Interconnected Amorphous NiFe Layered Double Hydroxides for Boosting Oxygen Evolution Reaction

Zhuo Chen , Qiang Qu , Xinsheng Li , Katam Srinivas , Yuanfu Chen * , Ming-qiang Zhu *

Posted Date: 8 October 2023

doi: 10.20944/preprints202310.0434.v1

Keywords: Room-temperature synthesis; layered double hydroxides; carbon nanotubes; NiFe-LDH@CNT; oxygen evolution reaction.

Article

Room-Temperature Synthesis of Carbon Nanotubes-Interconnected Amorphous NiFe Layered Double Hydroxides for Boosting Oxygen Evolution Reaction

Zhuo Chen [1,†], Qiang Qu [1,†], Xinsheng Li [2], Katam Srinivas [2], Yuanfu Chen [2,*] and Mingqiang Zhu [1,*]

[1] College of Mechanical and Electronic Engineering, Northwest A&F University, Yangling 712100, PR China
[2] School of Integrated Circuit Science and Engineering, and State Key Laboratory of Electronic Thin Films and Integrated Devices, University of Electronic Science and Technology of China, Chengdu 610054, PR China
* Correspondence: yfchen@uestc.edu.cn (Y.C.), zmqsx@nwsuaf.edu.cn (M.Z.)
† These authors contributed equally to this work.

Abstract: Oxygen evolution reaction (OER) is a key half-reaction in electrocatalytic water splitting. Large-scale water electrolysis is hampered by the commercial precious metal-based OER electrocatalysts owing to their high cost and slow kinetics. To address these issues, we present a facile one-pot room-temperature coprecipitation method to quickly synthesize carbon nanotubes-interconnected amorphous NiFe-layered double hydroxides (NiFe-LDH@CNT) as low-cost, efficient and stable OER electrocatalyst. The hybrid catalyst NiFe-LDH@CNT delivers outstanding OER performance with a low onset overpotential of 255 mV and a small Tafel slope of 51.2 mV dec^{-1}, as well as outstanding long-term stability. The terrific catalytic capability of NiFe-LDH@CNT can be associated with the synergistic effects of its room-temperature synthesized amorphous structure, bi-metallic modulation, and conductive CNT skeleton. The room-temperature synthesis can not only offer economic feasibility, but also obtain amorphous NiFe-LDH without crystalline boundaries, facilitating long-term stability during OER process. The bi-metallic nature of NiFe-LDH guarantees a modified electronic structure, providing additional catalytic sites. Simultaneously, the highly conductive CNT network fosters a nanoporous structure, facilitating electron transfer, O_2 release and enriching catalytic sites. This study presents a strategy to purposefully design nanoarchitecture and facilely synthesize amorphous transition metal-based OER catalysts, ensuring the cost effectiveness, production efficiency, and long-term stability.

Keywords: room-temperature synthesis; layered double hydroxides; carbon nanotubes; NiFe-LDH@CNT; oxygen evolution reaction

1. Introduction

The extensive consumption of traditional energy resources and their environmental impact have propelled the significant exploration of renewable energy technologies in recent years [1]. One particular area of interest is electrochemical water splitting, which becomes one of the most promising approaches to obtain clean hydrogen energy[2]. Oxygen evolution reaction (OER) plays a crucial role during electrocatalytic water splitting. However, large-scale water electrolysis is hindered by the slow kinetics of OER [3,4]. So, it is urgent to develop highly efficient and stable catalysts to mitigate the reaction barrier of OER.

Although commerical noble metal-based catalysts exhibit outstanding OER performance [5–7], the widespread utilization of these catalysts is constrained by their high cost, scarcity, and toxicity. Recently, non-precious transition metal-based compounds have emerged as promising electrocatalysts for OER [8]. Among them, NiFe-based layered double hydroxides (LDH) have gained

 doi:10.20944/preprints202310.0434.v1

great attention, especially due to the disparity in electron affinity and ionic radius between Ni and Fe, which could create a local potential difference and facilitates reaction kinetics [9]. However, the synthesis method and catalytic activity of LDH catalysts should be significantly improved.

Generally, LDH can be synthesized via various methods such as hydrothermal reaction [10], solvothermal reaction [11], and coprecipitation method [12], at elevated temperatures for long time. Such synthesis involving elevated temperatures and extended durations, is energy-intensive and operationally complex, thus increasing production costs. So, it is necessary to develop a facile and rapid synthesis method at low temperature to solve the issues of high energy consumption, complicate operation and high production costs. In addition, the control of amorphous LDH structure during synthesis is very important because amorphous catalyst without crystalline boundaries generally has better long-term stability [13]. Electronic modulation and conductive skeleton have been considered as efficient strategies for catalytic performance enhancement. Bi-metallization of LDH delivers much better OER performance than mono-metallic LDH due to modulation of electronic structure and presence of richer active sites [14]. Several groups have reported that introducing conductive carbon nanomaterials can effectively mitigate the low conductivity issue of LDH thus improving OER performance [15–17]. However, it is still challengeable to combine a facile synthesis method and synergistic OER performance enhancement for LDH with low production cost, controllable crystalline nature, high efficiency and long-term stability.

To address such issues, herein, we present a facile one-pot room-temperature coprecipitation method to synthesize CNT-interconnected amorphous NiFe-LDH (NiFe-LDH@CNT) as efficient and stable OER catalyst. This room-temperature synthesis technology has several advantages such as rapid synthesis, economic feasibility, environmental sustainability and easy control of amorphous nature, compared to conventional LDH synthesis methods at elevated temperature for long time. Furthermore, the amorphous nature of NiFe-LDH facilitates long-term stability during OER process; the bi-metallic nature of NiFe-LDH guarantees a modified electronic structure with additional active sites; the highly conductive CNT network promotes nanoporous structure with enhanced surface area and rich catalytic sites and provides efficient conductive paths and a well-established interface between CNT and LDH. Due to the synergistic effects mentioned above, the amorphous NiFe-LDH@CNT catalyst delivers outstanding OER performance with a low onset overpotential of 255 mV and a small Tafel slope of 51.2 mV dec^{-1}, as well as a significant durability. This study presents a strategy to purposefully design nanoarchitecture and facilely synthesize amorphous transition metal-based OER catalysts, ensuring the cost effectiveness, production efficiency, and long-term stability.

2. Experimental Section

2.1. Materials

Nickel (II) nitrate hexahydrate ($Ni(NO_3)_2{\cdot}6H_2O$), iron(III) nitrate nonahydrate ($Fe(NO_3)_3{\cdot}9H_2O$), carbon nanotube paste (5% CNT in NMP), and ethanol were purchased from Aladdin, Co. Ltd. The Nafion solution was obtained from Shanghai Macklin Ltd. All chemical reagents were of analytical grade and utilized without any further purification. Distilled water (DI water with a resistivity of 18.2 MΩ cm) and ethanol served as the washing solvents throughout the entire investigation.

2.2. Synthesis

All transition metal-based layered double hydroxides samples in this work including monometallic Ni-LDH, Fe-LDH, bi-metallic NiFe-LDH, and the composite of NiFe-LDH and carbon nanotubes (NiFe-LDH@CNT) were synthesized via a facile coprecipitation method at room temperature. Nickel (II) nitrate, and/or iron(III) nitrate and dimethylimidazole (2 MI) as precursors, and the mixture of methanol and water acts as solution. Detailed synthesis methods of Ni-LDH, Fe-LDH, NiFe-LDH, and tNiFe-LDH@CNT are described as follows.

 doi:10.20944/preprints202310.0434.v1

2.2.1. Synthesis of Ni-LDH

Monometallic Ni LDH was synthesized by a coprecipitation reaction of nickel(II) nitrate with 2MI in a water-methanol solution at room temperature. In a typical procedure, 1168 mg of 2MI was dissolved in 70 mL of methanol, while 1453.95 mg of nickel(II) nitrate hexahydrate was dissolved in a mixed solution containing 56 mL of methanol and 14 mL of deionized water (DI). The two solutions were then mixed under continuous stirring for 10 minutes. The resulting mixture was left undisturbed for 4 h at room temperature. The obtained precipitate was subsequently filtered, washed two times using ethanol and water, followed by lyophilization. The obtained solid product was named as Ni-LDH and sealed for furhter characterizations and electrocatalytic activity test.

2.2.2. Synthesis of Fe-LDH

Monometallic Fe-LDH was synthesized at room temperature via a coprecipitation reaction of iron(III) nitrate and 2MI in a water-methanol solution. 1168 mg of 2MI was firstly dissolved in 70 mL of methanol, and 1399.25 mg of iron(III) nitrate nonahydrate was dissolved in a mixed solution containing 56 mL of methanol and 14 mL of DI water. The two solutions were then mixed under continuous stirring for 10 minutes. The resulting mixture was allowed to stand at room temperature for 4 hours without stirring. The precipitate was then filtered, washed with ethanol and DI water for two times at room temperature, and finally dried using a freeze dryer to obtain Fe-LDH.

2.2.3. Synthesis of NiFe-LDH

Bi-metallic NiFe-LDH (with a Ni:Fe molar ratio of 3:1) was synthesized at room temperature via a coprecipitation reaction of iron(III) nitrate and 2MI in a water-methanol solution. Firstly, 1168 mg of 2MI was dissolved in 70 mL of methanol; then 1090.46 mg nickel(II) nitrate hexahydrate and 349.81 mg of iron(III) nitrate nonahydrate were dissolved in a mixed solution containing 56 mL of methanol and 14 mL of DI water. The two solutions were then mixed under continuous stirring for 10 minutes. The mixture was left undisturbed for 4 h at room temperature. The precipitate was then filtered, washed with ethanol and DI water for two times at room temperature, and finally dried using a freeze dryer to obtain NiFe-LDH.

2.2.4. Synthesis of NiFe-LDH@CNT

Similar synthesis procedure of NiFe-LDH was adopted to prepare NiFe-LDH@CNT, except that 5 wt% CNT was uniformly dispersed in a mixture of methanol and water before adding iron(III) nitrate and nickel(II) nitrate with a Ni:Fe molar ratio of 3:1. In a typical procedure, 1168 mg of 2MI was dissolved in 70 mL of methanol; 2.8 g of CNT paste (5 wt% CNT in DMF solution) was added in a mixed solution containing 56 mL of methanol and 14 mL of DI water and the solution was rigorously stirred for at least 30 min to obtain uniform dispersion, and then 1090.46 mg nickel(II) nitrate hexahydrate and 349.81 mg of iron(III) nitrate nonahydrate were dissolved in the mixed solution of water, ethenol and CNT; subsequently, the 2MI solution and the solution with nickel(II) nitrate, iron(III) nitrate and CNT were mixed under continuous stirring for 10 minutes. The mixture was left undisturbed for 4 h at room temperature. The precipitate was then filtered, washed with ethanol and DI water for two times at room temperature, and finally dried using a freeze dryer to obtain NiFe-LDH@CNT.

2.2. Structural Characterizations

The X-ray diffraction (XRD) patterns of of CNT, NiFe-LDH, and NiFe-LDH@CNT were examined by using a Bruker D8 Advance powder X-ray diffractometer, equipped with a Co Kα radiation source with a wavelength of 1.79026Å (at 40.0 kV and 40.0 mA). The scan range is from 10° to 80° with a scan rate of 4°/min. Confocal Laser Raman microscope (Renishaw Corporation, excitation at 532 nm) was used to analyze the Raman spectrum of NiFe-LDH@CNT sample. Scanning electron microscopy (SEM) images were performed by Hitachi SU8020 microscope (Hitachi Ltd., Tokyo, Japan). Transmission electron microscopy (TEM), High-resolution transmission electron

 doi:10.20944/preprints202310.0434.v1

microscopy (HRTEM), Selected area electron diffraction (SAED) and TEM-EDS were employed to probe the microstructure of materials, using FEI Tecnai G2 F30 (FEI Ltd., Hillsboro, USA) and XPLORE (Oxford Instruments). The accelerating voltages for TEM imaging and TEM-EDS mapping were 300 kV. The X-ray photoelectron spectroscopy (XPS) was performed by using an ESCALAB 250XI (Thermo Fisher Scientific Inc., Waltham, MA, USA) with Al Kα radiation (1486.6 eV photon energy) as the excitation source. Binding energies were referenced to the C 1s peak with the minimum binding energy (284 eV).

2.3. Electrochemical Characterizations

Electrochemical investigations were conducted using a CHI-660D electrochemical workstation (CH Instruments Co., Ltd., Shanghai, China). The three-electrode system consisted of a reference electrode (Hg/HgO electrode, CHI152), a counter electrode (graphite rod), and a working electrode (catalyst-modified glassy carbon electrode or GCE).

To prepare the working electrode, the glassy carbon electrode was first sonicated in an ethanol environment for 15 minutes and then polished with Al_2O_3 (0.05 μm) for 10 minutes. The catalyst ink was prepared by mixing 750 μL of deionized water, 250 μL of ethanol, 50 uL of a 5 wt% Nafion solution (DuPont Co., Delaware, USA), and 4 mg of different catalyst samples. Next, 5 μL of the well-dispersed catalyst ink was dropped onto the centre of the pre-treated GC electrode. The working electrode was then slowly dried in a baking oven at 60 °C until a layer of catalyst film attached to the centre. After cooling to room temperature, the electrochemical tests were initiated.

The potential measurements were converted to the reversible hydrogen electrode (RHE) potential using the conversion relationship: E vs. RHE = E vs. Hg/HgO + 0.0592 × pH + 0.098. The pH value of the 1.0 M KOH electrolyte, measured by the pH meter PHS-3E was found to be 13.96. For linear sweep voltammetry (LSV) tests, scans were conducted from 0.923 to 1.722 V versus RHE at a scan rate of 5 mV/s after conducting cyclic voltammetry for 20 cycles at 0.1 V/s. Electrochemical impedance spectroscopy (EIS) was performed at a potential corresponding to a current density of 10 mA/cm^2, ranging from 1.0 × 10^{-3} to 1.0 × 10^{-5} Hz. The electrochemically active surface area tests were based on the double-layer capacitance theory using the cyclic voltammetry (CV) method. The measurements were conducted from 0.35 to 0.45 V versus RHE at scan rates of 20-200 mV/s. Stability tests consisted of two parts: chronopotentiometry measurements recorded at current densities of 10 mA/cm^2 and cyclic voltammetry measurements involving 1000 cycles of CV. Foam nickel (NF, 1 cm × 1 cm) was used as the load material in these tests. Since the electrolyte concentration was high (1 M KOH), no IR compensation was considered in all polarization curves.

3. Results and Discussion

3.1. Synthesis and Structural Characterizations

As schematically illustrated in Figure 1, Ni-LDH, Fe-LDH, NiFe-LDH, and NiFe-LDH@CNT samples were prepared by a facile one-pot co-precipitation approach at room-temperature. CNT slurry was used to bulid a functional network with excellent conductivity, stable structure, and high reaction activity.

In order to analyze the crystalline structures of samples, X-ray diffraction (XRD) patterns of NiFe-LDH@CNT, NiFe-LDH, and commercial carbon nanotubes were conducted. As shown in Figure 2a, the CNT sample shows a clear (002) peak near around 26° and there were a few weak peaks appeared on the pattern of NiFe-LDH, indicating its lack of discernible crystalline structures; as for NiFe-LDH@CNT, a characteristic peak around 26° can be indexed as (002) peak of CNT, and there are nearly no obvious peaks for NiFe-LDH, indicating its amorphous nature or lack of discernible crystalline structures, which is mainly attributed to the low-temperature synthesis at room temperature. The amorphous nature of NiFe-LDH in NiFe-LDH@CNT means lack of crystalline boundaries, which suggests that NiFe-LDH@CNT might be more stable in alkaline electrolytes during OER, comparable to crystalline sample. The Raman spectrum of NiFe-LDH@CNT was characterized. As shown in Figure 2b, three characteristic peaks of at 1350.3, 1574.0, 2690.5 cm^{-1}

Preprints (www.preprints.org) | NOT PEER-REVIEWED | Posted: 8 October 2023 doi:10.20944/preprints202310.0434.v1

correspond to D, G, and 2D bands of CNT. A large I_D/I_G ratio of 1.26 and a distinct 2D peak in the Raman spectrum, indicate the presence of significant lattice defects and a higher degree of graphitization after 5% CNT incorporation. It suggests that the NiFe-LDH@CNT could have more active sites and high conductivity.

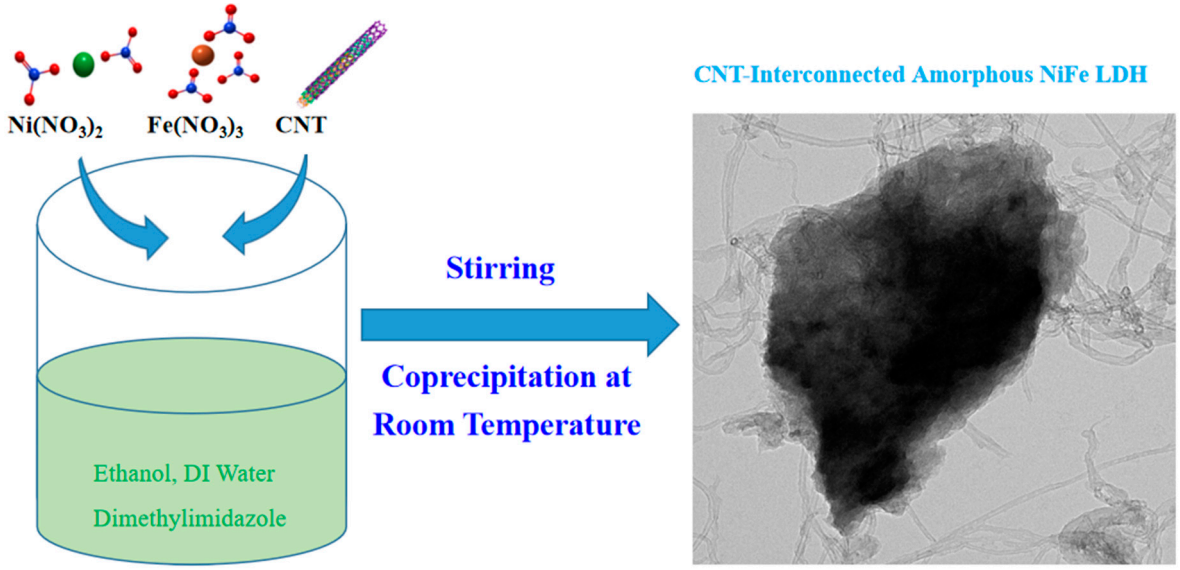

Figure 1. Schematic illustration of NiFe-LDH@CNT fabrication.

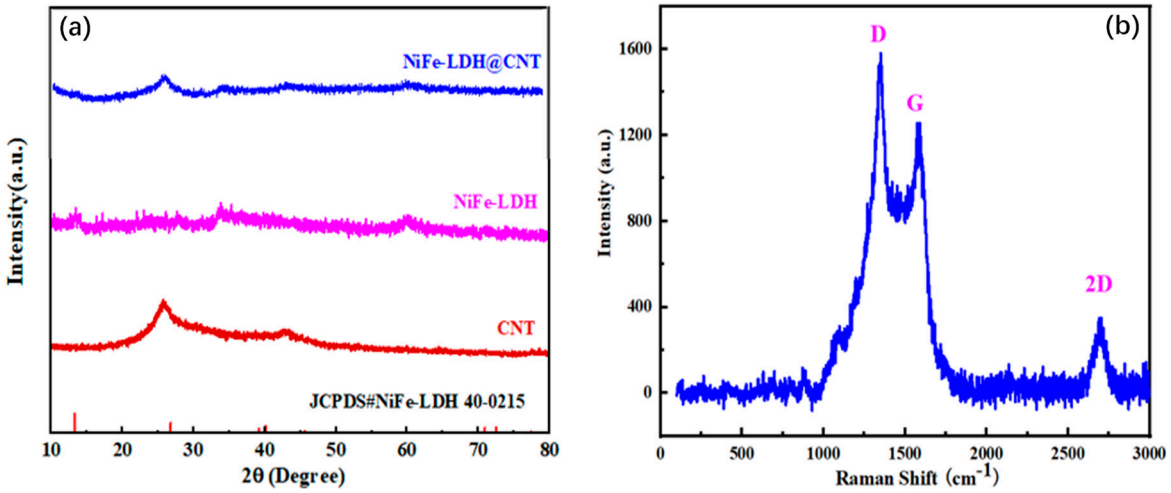

Figure 2. (a) XRD patterns of NiFe-LDH@CNT, NiFe-LDH, and commercial CNT. (b) Raman spectrum of NiFe-LDH@CNT.

X-ray photoelectron spectroscopy (XPS) was employed to gain insights into the surface microstructure and chemical composition of NiFe-LDH@CNT. As shows in Figure 3a, the characteristic peaks of Ni, Fe, O, and C elements appear in the survey spectrum of NiFe-LDH@CNT, which confirms the co-existence of these elements. The high-resolution Ni 2p, Fe 2p, and C 1s spectra of NiFe-LDH@CNT were illustrated in Figure 3b-d, respectively, with corresponding peak fitting data summarized in Table S1.

Preprints (www.preprints.org) | NOT PEER-REVIEWED | Posted: 8 October 2023 doi:10.20944/preprints202310.0434.v1

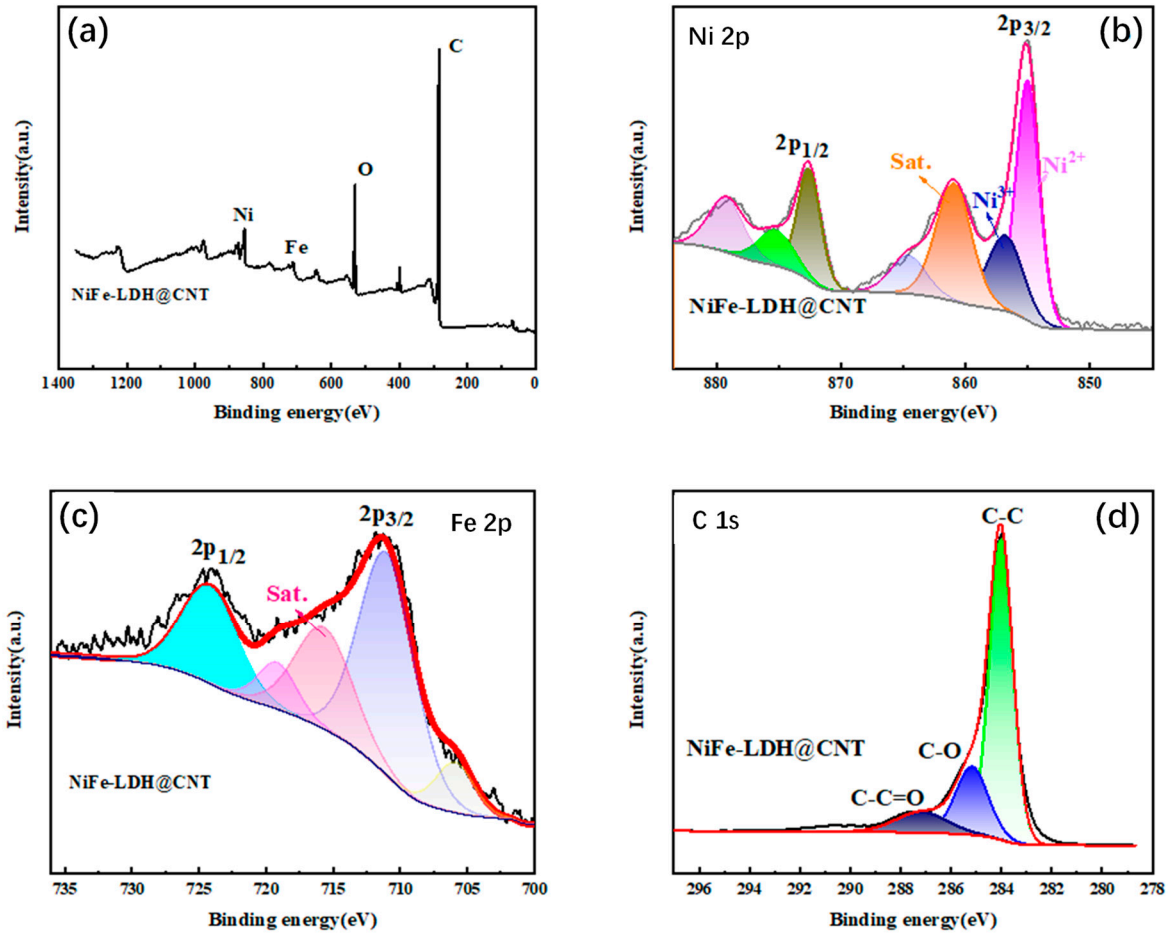

Figure 3. XPS spectral data of Ni-Fe LDH@CNT: (a) survey spectrum, and high-resolution spectra of (b) Ni 2p, (c) Fe 2p, and (d) C 1s, respectively.

XPS spectra of Ni and Fe elements can be split into two doublet components ($2p_{3/2}$ and $2p_{1/2}$), as a result of spin-orbit coupling. Figure 3b-c illustrate that for NiFe-LDH@CNT, Ni ions are predominantly resided in the oxidation state of Ni $^{2+}$, while Fe ions are primarily occupied the +3 oxidation state. Wherein the peaks located at 854.99 and 872.52 eV represent the Ni^{2+} state and the other peaks at 856.40 and 874.68 eV denote the Ni^{3+} state, and these are accompanied by three satellite peaks located at around 860.80, 863.46 and 879.03 eV. Similarly, during the fitting analysis of the Fe 2p peak shown in Figure 3c, a characteristic pair of peaks were observed at binding energies near 710.72 and 724.15 eV, assigned to Fe^{3+} states with electron configurations of $2p_{3/2}$ and Fe^{3+} states with electron configurations of $2p_{1/2}$ respectively. Importantly, a distinct low-intensity peak was observed preceding the $2p_{3/2}$ peak, indicating the presence of lower oxidation state Fe ions in the vicinity (Figure 3c). This is very consistent with previous research [18,19]. The valence states on the material's surface were found to be unaffected by the presence of CNT networks. This finding was further supported by high-resolution spectrum of C1s (Figure 3d).

Further characterization of the surface morphology and structural features of NiFe-LDH@CNT was carried out by Scanning Electron Microscope (SEM) and Transmission Electron Microscope (TEM). Figure 4a-b present the SEM and TEM images, highlighting the presence of carbon nanotubes and NiFe-LDH particles. The high-resolution TEM (HR-TEM) image of NiFe-LDH@CNT was performed. As shown in Figure 4c, one can clearly observe that the NiFe-LDH nanoparticle was interconnected by many carbon nanotubes. This interconnection suggests the successful intergration of conductive carbon nanotubes, which is anticipated to effectively facilitate the electron transfer in the NiFe-LDH@CNT composite. Figure 4d-g shows the morphology and corresponding elemental mapping images. The consistence between the morphology and element mapping indicates a high level of uniformity and ordered atomic arrangement at the nanoscale.

Preprints (www.preprints.org) | NOT PEER-REVIEWED | Posted: 8 October 2023 doi:10.20944/preprints202310.0434.v1

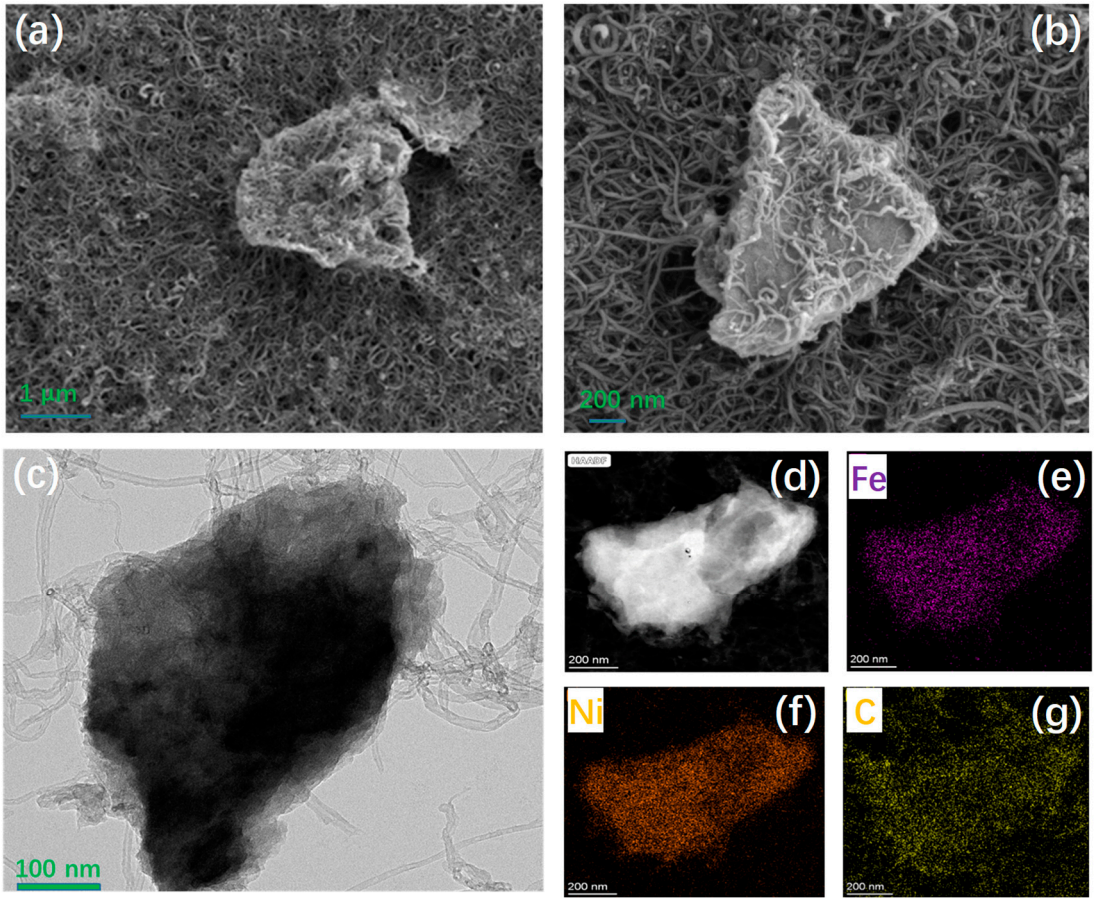

Figure 4. (a) SEM, (b) TEM, (c) HR-TEM, and the (d-g) Elemental mapping images of NiFe-LDH@CNT.

3.2. Oxygen Evolution Activity

To assess the OER performance of the as-synthesized catalysts, a standard three-electrode setup with a 1.0 M KOH electrolyte was utilized. Initially, the activated glassy carbon electrode (GCE) was employed for linear sweep voltammetry (LSV) testing, which offers the insights into catalytic activity, reaction mechanisms, and electrocatalytic performance of the materials [20]. During electrochemical reactions, chemical reactions occured on the surface of material when an external potential is applied [21]. As shown in Figure 5a, when a fixed potential (particularly larger than 1.6 V) is applied, NiFe-LDH can obtain larger current density than those of Ni-LDH, Fe-LDH, which suggests bi-metallization can improve the catalytic activity. Furthermore, the incorporation of conductive CNT in NiFe-LDH@CNT results in a much higher current density than that of NiFe-LDH, confirming that after introducing conductive carbon nanotubes, the catalytic activity is significantly enhanced. The onset overpotentials at 1 mA cm^{-2} for Ni-LDH, Fe-LDH, NiFe-LDH, and NiFe-LDH@CNT are 329, 307, 282, and 255 mV, respectively. Obviously, compared to monometallic LDHs of Ni-LDH (329 mV) and Fe-LDH(307 mV), bimetallic NiFe-LDH has a much lower onset overpotential (282 mV), suggesting that bi-metallization is beneficial to decrease the overpotential due to modification of electronic structure. Furthermore, one can observe that compared to NiFe-LDH, the onset overpotential of NiFe-LDH@CNT can be significantly decreased. Similarily, to achieve the benchmark current density of 10 $mAcm^{-2}$, NiFe-LDH@CNT requires a much smaller overpotential (η_{10} = 330 mV) over the other samples (448 mV for Ni-LDH, 419 mV for Fe-LDH, and 369 mV for NiFe-LDH). It indicates that the excellent OER activity could be owing to the synergistic effect of bi-metallization and the introduction of conductive CNTs network.

Preprints (www.preprints.org) | NOT PEER-REVIEWED | Posted: 8 October 2023 doi:10.20944/preprints202310.0434.v1

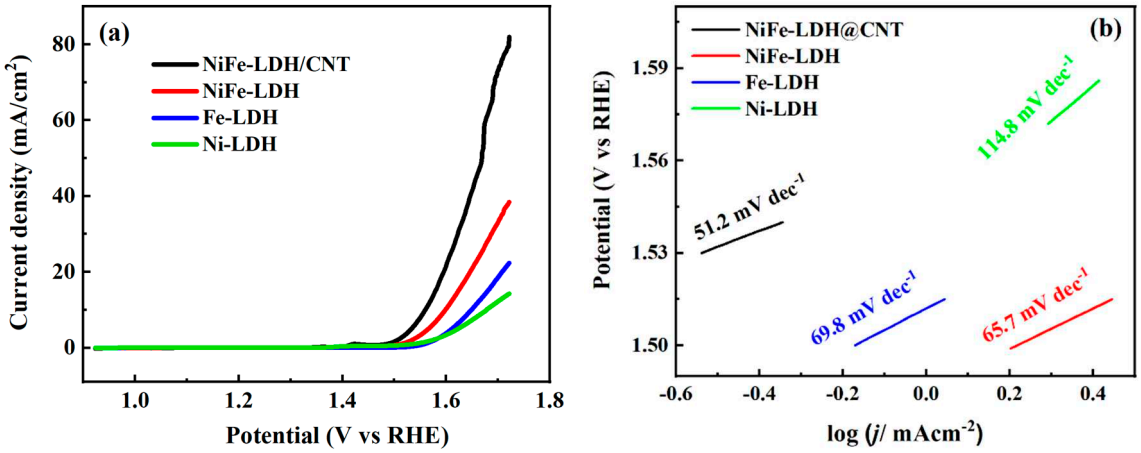

Figure 5. (a) LSV curves and (b) Tafel slopes of NiFe-LDH@CNT, NiFe-LDH, Fe-LDH, and Ni-LDH.

To gain a deeper understanding, Tafel slope calculations were conducted using the LSV data. The Tafel slope offers insights into reaction feasibility, which can be calculated from either the Tafel equation ($\eta = a + b \times \log(j)$) or ($E = a_1 + b \times \log(j)$). According to the widely acknowleged mechanism, the electrocatalytic efficiency of OER is closely associated with the energy barriers encountered during the conversion of OH* to O* and O* to OOH* [22]. The Tafel slope, as determined by applying the *Butler-Volmer* theory, serves as an indicator for identifying the rate-determining step in each reaction stage [23]. Tafel slope can be used to further assess the OER kinetics. As shown in Figure 5b, it is evident that compared to monometallic LDHs of Ni-LDH (114.8 mV dec^{-1}) and Fe-LDH(69.8 mV dec^{-1}), bimetallic NiFe-LDH has a lower Tafel slope (65.7 mV dec^{-1}), suggesting that bi-metallization facilitate to decrease Tafel slope. After introducing carbon nanotubes, NiFe-LDH@CNT exhibits an extraordinarily low Tafel slope of 51.2 mV•dec^{-1}, which is obviously better than NiFe-LDH (65.7 mV dec^{-1}). This result demonstrats that combining the bi-metalization and conductive skeleton stratedgy, superior intrinsic catalytic activity of NiFe-LDH@CNT can be obtained.

To accurately depict the alterations in the material, we conducted measurements of the electrochemical active surface area (ECSA) within a potential window devoid of Faradaic processes. Generally, the elevated values of double-layer capacitance (C_{dl}) indicate an increased ECSA, which corresponds to a greater number of active sites and more robust OER process [24]. The C_{dl} values of Ni-LDH, Fe-LDH, NiFe-LDH, and NiFe-LDH@CNT can be calculated using the CV curves (Figure S1). As shown in Figure 6a, the C_{dl} values of Ni-LDH, Fe-LDH, NiFe-LDH and NiFe-LDH@CNT are 0.66, 1.01, 2.27, and 2.56 mF cm^{-2}, respectively. One can observe that compared to monometallic LDHs of Ni-LDH (0.66 mF cm^{-2}) and Fe-LDH(0.66 mF cm^{-2}), bimetallic NiFe-LDH shows much larger C_{dl} value (2.27 mF cm^{-2}), which suggests that bi-metallization generates many more active sites; compared to NiFe-LDH, the C_{dl} value of NiFe-LDH@CNT is further increased. It can be explained that the introduction of carbon nanotubes and the interconnection between NiFe-LDH and carbon nanotubes further generate additional active sites. Among these samples, NiFe-LDH@CNT possesses the highest C_{dl} value of 2.56 mF cm^{-2}, confirming that it will have the best OER performance.

Subsequently, the electrochemical impedance spectroscopy (EIS) was investigated for assessing the reaction kinetics. As shown in Figure 5b, the EIS plot was fitted using Z-View software. The semicircle diameters of the EIS plots which represent the values of charge transfer resistance (R_{ct}), show the complexity and kinetics of the reaction. Notably, NiFe-LDH@CNT substantially displays the lower R_{ct} value compared to the other samples, implying faster charge transfer rates, which is consistent with observations from the Tafel curves (as depicted in Figure 4b). Specifically, the R_{ct} values of Ni-LDH, Fe-LDH, NiFe-LDH and NiFe-LDH@CNT are 129.08, and 69.25, 57.24, and 55.93 Ω, respectively. It is obvious that bimetallic NiFe-LDH shows the lower R_{ct} values than those of Ni-LDH or Fe-LDH. This superiority may be due to that the synergistic interactions between Ni and Fe could results in a relatively loose electronic structure and low resistivity. Compared to NiFe-LDH, NiFe-LDH@CNT displays a smaller value of R_{ct} (55.93 Ω), which indicates that the highly conductive

Preprints (www.preprints.org) | NOT PEER-REVIEWED | Posted: 8 October 2023 doi:10.20944/preprints202310.0434.v1

CNT interconnected bimetallic LDH composite enabling faster charge transfer and better OER performance. This shows that NiFe-LDH@CNT has a good potential for practical application.

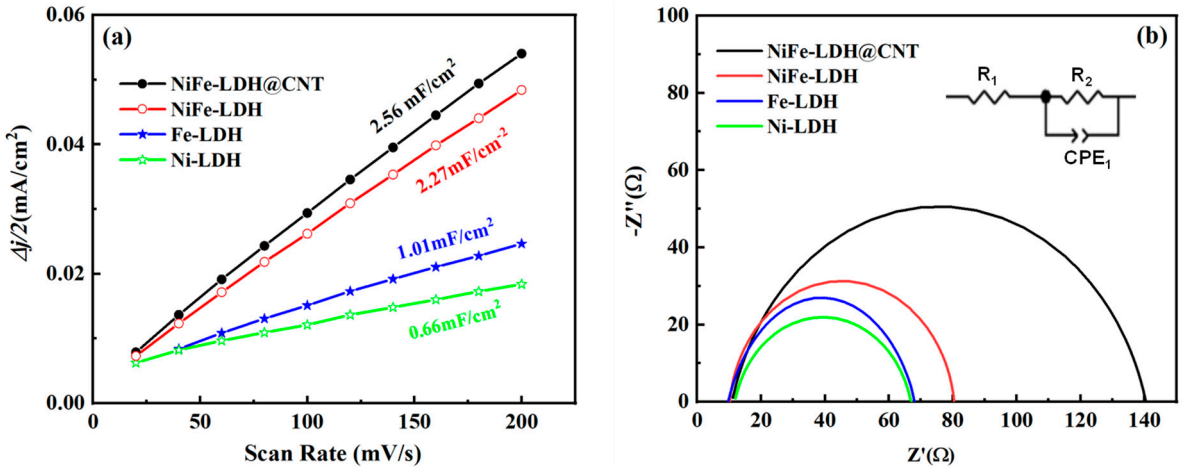

Figure 6. (a) C_{dl} data and (b) EIS spectra of Ni-LDH, Fe-LDH, NiFe-LDH, and NiFe-LDH@CNT.

The stability of the electrocatalyst in harsh alkaline conditions is crucial for practical applicability. The stability tests of NiFe-LDH@CNT catalyst were conducted. Figure 7a shows the CV curves of NiFe-LDH@CNT onto a GC electrode before and after 1000 cycles. It suggests that when the potential is higher than 1.5 V, only a minimal degradation is observed, indicating its stable electrocatalytic activity. Moreover, the chronoamperometric test was carried out by depositing the catalyst ink onto a nickel foam. As shown in Figure 7b, at a fixed voltage of 0.604 V, the current density retention could be up to 94.45% after 24 h, suggesting excellent long-term stability during OER process in alkaline solution. The excellent catalytic activity and good stability of NiFe-LDH@CNT suggests its potential for practical applications.

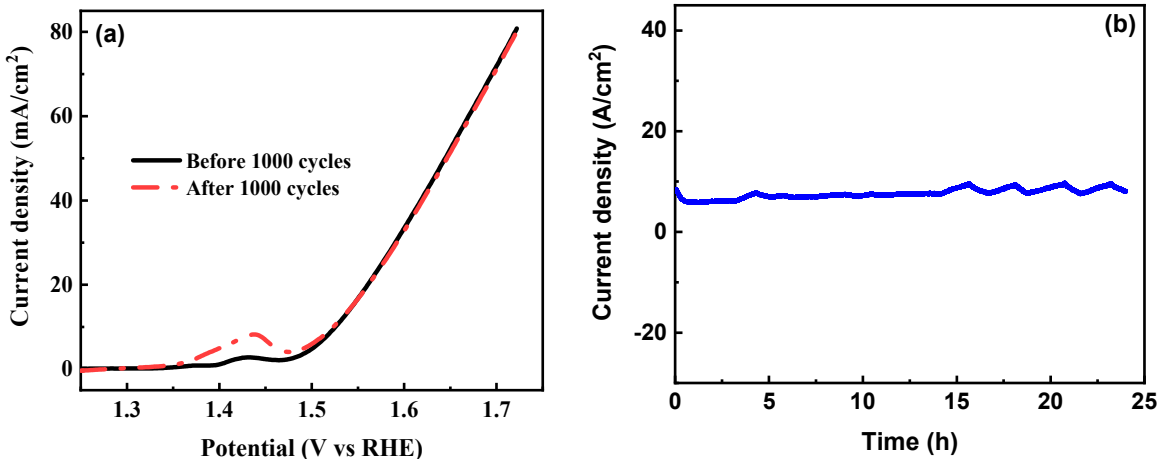

Figure 7. Stability of NiFe-LDH@CNT. (a) LSV cures before and after 1000 cycles. (b) *I-t* test at a fixed voltage of 0.604 V.

3. Conclusions

In order to effectively boost the OER performance of transition metal-based layered double hydroxides, we present a synergistic approach by combining the crystalline structure control via synthesis condition and OER performance enhancement strategy of electronic structure modification via bi-metallization and construction of conductive skeleton. A facile one-pot co-precipitation approach was successfully developed to swiftly synthesize amorphous NiFe layered double hydroxides interconnected with carbon nanotubes (NiFe-LDH@CNT) at room temperature. This

room-temperature synthesis not only offers a cost-effective and environmentally sustainable approach, but also allows for the advantageous amorphous structure of NiFe-LDH without distinct crystalline boundaries. This structural characteristic significantly contributes to the long-term stability observed during the OER. The bimetallic composition of NiFe-LDH plays a vital role in modifying the electronic configuration and creating the additional catalytic sites. Furthermore, the integration of carbon nanotubes (CNT) aids in forming a nanoporous structure, enabling efficient ion diffusion and oxygen release. The highly conductive network of carbon nanotubes provides an effectively conductive paths and establishes a well-structured interface with layered double hydroxides, facilitating electron transfer. The combined advantages of these structural and compositional aspects culminate in outstanding OER performance of LDH sample name, exemplified by a minimal onset overpotential of 255 mV, an impressively low Tafel slope of 51.2 mV dec^{-1}, and significant long-time operability. In summary, this work not only introduces a strategy for designing a well-considered nanoarchitecture, but also offers a facile synthesis route to achieve non-precious metal-based amorphous structures for OER catalysis. This approach holds the great promise, and presents the stable OER catalysts with economically viable and highly efficient, and for practical applications.

Supplementary Materials: The following supporting information can be downloaded at the website of this paper posted on Preprints.org. Figures S1: Voltammograms of Ni-LDH, Fe-LDH, NiFe-LDH, and NiFe-LDH@CNT; Table S1: The fitted peak data of XPS of NiFe-LDH@CNT.

Author Contributions: Zhuo Chen and Qiang Qu: Conceptualization, Investigation, Methodology, Formal analysis, Writing – original draft. Xingsheng Li: Data curation, Formal analysis, Data fitting. Katam Srinivas: Writing – review & editing. Yuanfu Chen and Ming-qiang Zhu: Supervision, Funding acquisition, Project administration, Formal analysis, Resources, Writing – review & editing.

Funding: The research was financially supported by National Undergraduate Training Program for Innovation and Entrepreneurship (Grant No. S202310712007), Natural Science Foundation of Sichuan Province of China (Grant No. 2023NSFSC0084), and National Natural Science Foundation of China (Grant No. 21773024).

Institutional Review Board Statement: Not applicable.

Informed Consent Statement: Not applicable.

Data Availability Statement: The data were available on request from the corresponding authors.

Conflicts of Interest: The authors declare no conflict of interest.

References

1. Chu, S; Majumdar, A., Opportunities and challenges for a sustainable energy future. Nature **2012**, 488, 294–303.
2. Wang, B.; Srinivas, K.; Wang, X.; Su, Z.; Yu, B.; Zhang, X.; Liu, Y.; Ma, F.; Yang, D.; Chen, Y., Self-assembled CoSe2-FeSe2 heteronanoparticles along the carbon nanotube network for boosted oxygen evolution reaction. *Nanoscale* **2021,** 13, 9651-9658.
3. Karmakar, A.; Karthick, K.; Kumaravel, S.; Sankar, S. S.; Kundu, S., Enabling and Inducing Oxygen Vacancies in Cobalt Iron Layer Double Hydroxide via Selenization as Precatalysts for Electrocatalytic Hydrogen and Oxygen Evolution Reactions. *Inorg. Chem.* **2021,** 60, 2023-2036.
4. Najafpour, M. M.; Allakhverdiev, S. I., Manganese compounds as water oxidizing catalysts for hydrogen production via water splitting: From manganese complexes to nano-sized manganese oxides. *Int. J. Hydrog. Energy* **2012,** 37, 8753-8764.
5. Lyu, F. L.; Wang, Q. F.; Choi, S. M.; Yin, Y. D., Noble-Metal-Free Electrocatalysts for Oxygen Evolution. *Small* **2019,** 15, 17.
6. Saha, S.; Ganguli, A. K., FeCoNi Alloy as Noble Metal-Free Electrocatalyst for Oxygen Evolution Reaction (OER). *ChemistrySelect* **2017,** 2, 1630-1636.
7. Tan, D. M.; Xiong, H.; Zhang, T.; Fan, X. L.; Wang, J. J.; Xu, F., Recent progress in noble-metal-free electrocatalysts for alkaline oxygen evolution reaction. *Front. Chem.* **2022,** 10, 10.
8. Evans, D. G.; Slade, R. C. T., Structural aspects of layered double hydroxides. In *Layered Double Hydroxides*, Duan, X.; Evans, D. G., Eds. Springer-Verlag Berlin: Berlin, **2006,** 119, 1-87.
9. Qin, X.; Teng, J.; Guo, W. Y.; Wang, L.; Xiao, S. N.; Xu, Q. J.; Min, Y. L.; Fan, J. C., Magnetic Field Enhancing OER Electrocatalysis of NiFe Layered Double Hydroxide. *Catal. Lett.* **2023,** 153, 673-681.

10. Xu, X.; Zhong, Z.; Yan, X. M.; Kang, L. T.; Yao, J. N., Cobalt layered double hydroxide nanosheets synthesized in water-methanol solution as oxygen evolution electrocatalysts. *Journal of Materials Chemistry A* **2018,** 6, 5999-6006.
11. Souleymen, R.; Wang, Z. T.; Qiao, C.; Naveed, M.; Cao, C. B., Microwave-assisted synthesis of graphene-like cobalt sulfide freestanding sheets as an efficient bifunctional electrocatalyst for overall water splitting. *Journal of Materials Chemistry A* **2018,** 6, 7592-7607.
12. Gang, C. A.; Chen, J. Y.; Chen, Q. H.; Chen, Y. T., Heterostructure of ultrafine FeOOH nanodots supported on CoAl-layered double hydroxide nanosheets as highly efficient electrocatalyst for water oxidation. *J. Colloid Interface Sci.* **2021,** 600, 594-601.
13. Ye, Y.; Shan, Y.; Zhu, H.; Chen, K.; Yu, X., Controllable formation of amorphous structure to improve the oxygen evolution reaction performance of a CoNi LDH. *Rsc Advances* **2023,** 13, 2467-2475.
14. Lu, X. Y.; Xue, H. R.; Gong, H.; Bai, M. J.; Tang, D. M.; Ma, R. Z.; Sasaki, T., 2D Layered Double Hydroxide Nanosheets and Their Derivatives Toward Efficient Oxygen Evolution Reaction. *Nano-Micro Lett.* **2020,** 12, 32.
15. Liu, Z. B.; Yu, C.; Han, X. T.; Yang, J.; Zhao, C. T.; Huang, H. W.; Qiu, J. S., CoMn Layered Double Hydroxides/Carbon Nanotubes Architectures as High-Performance Electrocatalysts for the Oxygen Evolution Reaction. *ChemElectroChem* **2016,** 3, 906-912.
16. Wu, L.; Yu, L.; Zhang, F.; Wang, D.; Luo, D.; Song, S.; Yuan, C.; Karim, A.; Chen, S.; Ren, Z., Facile synthesis of nanoparticle-stacked tungsten-doped nickel iron layered double hydroxide nanosheets for boosting oxygen evolution reaction. *Journal of Materials Chemistry A* **2020,** 8, 8096-8103.
17. Liu, Z.; Yu, C.; Han, X.; Yang, J.; Zhao, C.; Huang, H.; Qiu, J., CoMn Layered Double Hydroxides/Carbon Nanotubes Architectures as High-Performance Electrocatalysts for the Oxygen Evolution Reaction. *ChemElectroChem* **2016,** 3, 906-912.
18. Yan, L.; Xu, Z. Y.; Liu, X. A.; Mahmood, S.; Shen, J. L.; Ning, J. Q.; Li, S.; Zhong, Y. J.; Hu, Y., Integrating trifunctional Co@NC-CNTs@NiFe-LDH electrocatalysts with arrays of porous triangle carbon plates for high-power-density rechargeable Zn-air batteries and self-powered water splitting. *Chem. Eng. J.* **2022,** 446, 11.
19. Huang, L.; Wu, H.; Liu, H.; Zhang, Y., Phosphorous doped cobalt-iron sulfide/carbon nanotube as active and robust electrocatalysts for water splitting. *Electrochim. Acta* **2019,** 318, 892-900.
20. Diard, J. P.; Le Gorrec, B.; Montella, C., Diffusion layer approximation under transient conditions. *Journal of Electroanalytical Chemistry* **2005,** 584, 182-191.
21. Wang, C.; Jin, L.; Shang, H.; Xu, H.; Shiraishi, Y.; Du, Y., Advances in engineering RuO2 electrocatalysts towards oxygen evolution reaction. *Chinese Chemical Letters* **2021,** 32, 2108-2116.
22. Fang, Y.-H.; Liu, Z.-P., Mechanism and Tafel Lines of Electro-Oxidation of Water to Oxygen on RuO2(110). *Journal of the American Chemical Society* **2010,** 132, 18214-18222.
23. Fletcher, S., Butler-Volmer meets microscopic reversibility. *Current Opinion in Electrochemistry* **2023,** 37.
24. Srinivas, K.; Chen, Y.; Su, Z.; Yu, B.; Karpuraranjith, M.; Ma, F.; Wang, X.; Zhang, W.; Yang, D., Heterostructural CoFe2O4/CoO nanoparticles-embedded carbon nanotubes network for boosted overall water-splitting performance. *Electrochim. Acta* **2022,** 404.